

Atomic micromotion and geometric forces in a triaxial magnetic trap

J. H. Müller, O. Morsch, D. Ciampini, M. Anderlini, R. Mannella, and E. Arimondo
 INFM, Dipartimento di Fisica, Università di Pisa, Via Buonarroti 2, I-56127 Pisa, Italy
 (October 28, 2018)

Non-adiabatic motion of Bose-Einstein condensates of rubidium atoms arising from the dynamical nature of a time-orbiting-potential (TOP) trap was observed experimentally. The orbital micromotion of the condensate in velocity space at the frequency of the rotating bias field of the TOP was detected by a time-of-flight method. A dependence of the equilibrium position of the atoms on the sense of rotation of the bias field was observed. We have compared our experimental findings with numerical simulations. The nonadiabatic following of the atomic spin in the trap rotating magnetic field produces geometric forces acting on the trapped atoms.

PACS number(s): 03.65.Bz, 32.80.Pj, 45.50.-j

Magnetic trapping has become a standard technique for confining and evaporatively cooling ultra-cold samples of neutral atoms. Up to now, BEC in alkali atoms has been achieved in two different kinds of magnetic traps: static traps, and dynamic ones, also called time-orbiting-potential (TOP) traps [1]. In the latter, introduced in [2], a quadrupole magnetic field is modified by a rotating homogeneous bias field which causes the quadrupole field to orbit around the origin, thus eliminating the zero of the magnetic field at the trap center. In the original scheme with cylindrical symmetry [2], the bias field rotates in the symmetry plane of the quadrupole field, whereas in a later version [3] the plane of rotation contains the quadrupole symmetry axis, which yields a completely asymmetric (triaxial) magnetic trap. In the present work, precise measurements on the motion of a ^{87}Rb condensate in the triaxial TOP trap have allowed us to discover new dynamical features, beyond the approximations previously applied in the theoretical treatment of time-dependent magnetic traps.

In the adiabatic approximation the spins of the magnetically trapped atoms follow the instantaneous direction of the magnetic field. Generally speaking, an adiabatic approximation is applied when the evolution of one set of variables of a system is fast compared to the time scale of a second one. While the full dynamics can be quite complicated and hard to analyze, in a useful approximation the fast motion is solved for fixed values of the slow coordinates, and then the slow dynamics is considered to be governed by the *average* values of the fast motion. In a classical description, the energy of the fast motion calculated for fixed values of the variables of the slow system acts as a potential in which the evolution of the slow system takes place. In an improved approxi-

mation, reaction forces act on the slow dynamics. They are related to the geometric phase and to the geometric gauge fields [4]. In the classical case, the physical origin of the geometric forces has been studied, e.g., for atomic systems with spins [5]. For atomic motion in an inhomogeneous magnetic field, the slow atomic external degree of freedom acts as a “guiding center” for the evolution of the fast precessing spin variables coupled to the magnetic field. The resulting geometric forces are usually very small and hard to detect. Analogous terms in the calculation of molecular spectra beyond the Born-Oppenheimer approximation do, however, lead to measurable shifts of energy levels, underlining the usefulness of the concept [4].

In the TOP trap, the guiding-center atomic motion within the time-dependent inhomogeneous magnetic field acquires an additional dynamic feature associated with the periodic evolution of the rotating field, feature not present in the analyses of [5]. Because the frequency of the bias field rotation is typically much larger than the vibrational frequencies of the atoms in the trap, in an additional approximation a time-average over the period of the rotating field is usually performed. Application of both adiabatic and time-average approximations predicts a description of the atomic motion in terms of a time-independent potential. A number of theoretical studies have considered the role of the nonadiabatic dynamics [6] or of the time-dependent potential on the atomic evolution in a TOP trap [7]. Experimental investigations, however, have restricted their attention mainly to the atomic response to the time-independent adiabatic potential.

The breakdown of the time-average approximation and of the adiabatic spin following approximation, and the evidence for additional geometric forces are visible in the following measurements on a ^{87}Rb condensate [8] in a triaxial trap: i) the atomic micromotion at the frequency of the bias field, ii) the change of the atomic equilibrium position in the trap when inverting the sense of rotation of the bias field [9], iii) the dependence of the rotation-sensitive equilibrium position on the applied magnetic fields. The dependence of the equilibrium position on the sense of rotation of the bias field does not violate any fundamental symmetry law, as the handedness of the Larmor precession for an atom in a trapped state defines the sense of rotation in the atomic evolution. In our experimental investigation, as for other TOP traps, the typical conditions for applying the adiabatic and time-averaged approximations are not violated [11]. A precise detection of the micromotion, however, allowed us to perform

measurements of the non-adiabatic effects present in the TOP trap. We have compared our results with analytical models and numerical simulations based on a completely classical description, obtaining good agreement.

Our experimental apparatus [12] is based on a double-MOT system with two cells connected by a glass tube to capture, cool and transfer atoms into a magnetic TOP trap. The latter consists of a pair of quadrupole coils oriented along a horizontal axis and two pairs of bias-field coils, one incorporated into the quadrupole coils and the other along a horizontal axis perpendicular to that of the quadrupole coils, as shown in Fig. 1. After transferring the atoms into the TOP-trap, we evaporatively cool them first by reducing the radius of the quadrupole orbit and finally by applying an RF-field. Once Bose-Einstein condensation has occurred in the $|F=2, m_F=2\rangle$ state, we adiabatically changed the quadrupole gradient and the bias field to the desired values. The instantaneous magnetic field seen by the atoms is:

$$\mathbf{B} = [2b'x + B_0 \cos \omega_0 t] \hat{\mathbf{i}} + [-b'y + B_0 \sin \omega_0 t] \hat{\mathbf{j}} - b'z \hat{\mathbf{k}} \quad (1)$$

where b' is the quadrupole gradient along the z -axis, and B_0 and ω_0 are the magnitude and the frequency of the bias field, respectively.

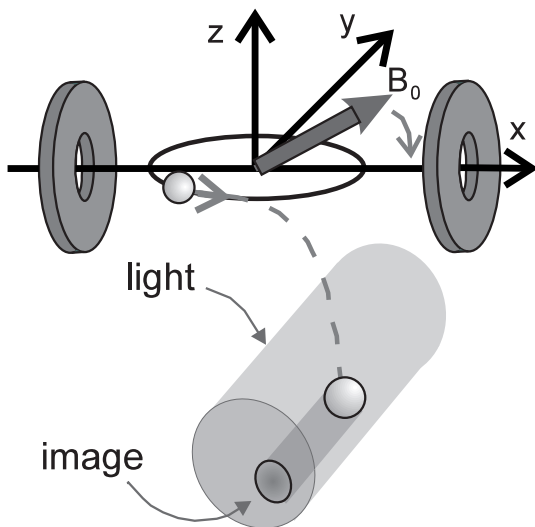


FIG. 1. Schematic of the static and rotating magnetic fields confining the condensate, and of the shadow-imaging method. Imaging along the y -axis allowed us to measure the velocity of the atoms along the x and z axes. For our trap parameters the spatial amplitude of the micromotion in the trap was less than $1 \mu\text{m}$, well below our resolution limit of $5 \mu\text{m}$.

Application of the adiabatic and time-average approximations leads to an oscillatory motion of the atoms in a time-independent potential with a harmonic frequencies $\omega_x : \omega_y : \omega_z$ of $2 : 1 : \sqrt{2}$, where $\omega_x = b' \sqrt{2\mu/mB_0}$, m being the mass and μ the magnetic moment of an atom in the trapped state [3]. Lifting the time-average approximation yields the atomic micromotion, because

the atoms experience a time-dependent potential at frequency ω_0 and its harmonics. Expansion of the potential energy U for atoms close to the trap center gives additional linear terms ΔU modulated at the frequency ω_0 on top of the effective harmonic potential, with

$$\Delta U = \mu b' (2x \cos \omega_0 t - y \sin \omega_0 t). \quad (2)$$

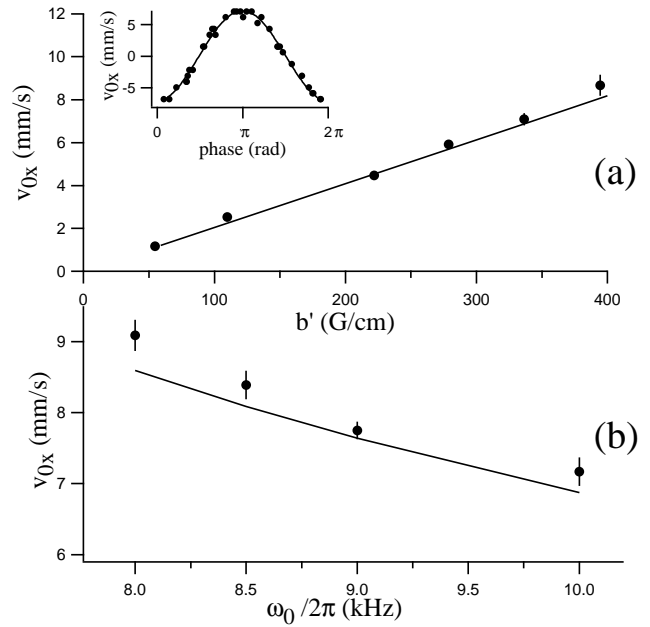


FIG. 2. Dependence of the micromotion velocity v_{0x} on b' at $\omega_0 = 2\pi \times 10^4 \text{ s}^{-1}$ in (a) and on ω_0 in (b). In (b), $b' = 329 \text{ Gcm}^{-1}$ and $B_0 = 28 \text{ G}$. In (a), for gradients larger than 200 Gcm^{-1} , $B_0 = 28 \text{ G}$ was used, whereas for smaller gradients B_0 was reduced in order to maintain a small gravitational sag. Continuous lines from Eqs. (3). The inset in (a) shows the velocity dependence on the phase of the bias field at which the trap was switched off (zero phase corresponds to the bias field pointing *along* the direction of observation).

For trap oscillation frequencies well below ω_0 , separation of the time scales allows us to write down the atomic micromotion at ω_0 as a small shaking motion on top of the secular motion in the trap. Balancing the restoring force from the ΔU potential with the centrifugal force of the resulting orbital motion yields a periodic micromotion with velocity amplitudes

$$v_{0x} = \frac{2\mu b'}{m\omega_0} \quad \text{and} \quad v_{0y} = \frac{\mu b'}{m\omega_0}. \quad (3)$$

In order to observe the micromotion of the atoms at the TOP-frequency, the trap fields were switched off in a time (less than $20 \mu\text{s}$) short compared to the period of the TOP-field [13]. The instant at which the trapping fields were switched off was determined to better than 1% of a TOP-cycle. After switching off the quadrupole field at

a well-defined phase of the rotating bias field and after a variable delay of up to 8 ms, we imaged the absorption shadow of the falling cloud onto a CCD-chip. Because of the small spatial amplitude of the micromotion, the measured position of the atoms along the x -axis after the time-of-flight was determined solely by their initial velocity v_{0x} in that direction (see Fig. 1).

A typical plot of v_{0x} as a function of the bias-field phase is shown in the inset of Fig. 2. A velocity amplitude of 5 mm s^{-1} corresponds to a spatial amplitude of the micromotion around 100 nm. Also shown in Fig. 2 is the dependence of v_{0x} on the quadrupole gradient and on the frequency of the rotating bias field. We found no dependence of v_{0x} on B_0 . All of these dependencies are in agreement with Eq. (3) (continuous lines in Fig. 2). We checked by numerical integration of the equations of motion in the adiabatic approximation that the finite switching time of the trapping field leads to a reduction of the measured micromotion velocity of at most a few percent compared to Eq. 3.

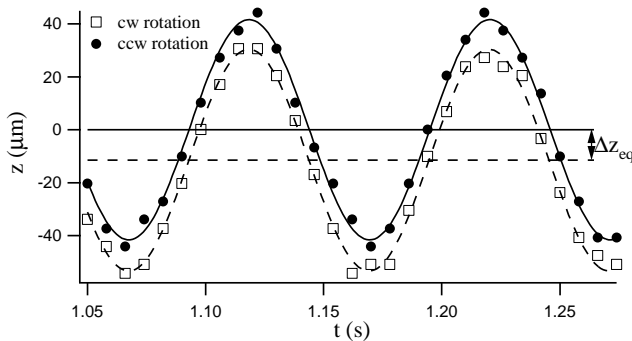


FIG. 3. Centre-of-mass oscillations of atoms in the TOP-trap for clockwise and counterclockwise rotation of the bias field. The gradient b' and the bias field B_0 were 20.8 G cm^{-1} and 4 G, respectively. The equilibrium positions for the two cases are indicated by the horizontal lines.

When the sense of rotation of the bias field was reversed, the phase of the measured velocity was shifted by 180 degrees, in accordance with the physical picture of the atoms being ‘dragged’ along by the instantaneous position of the quadrupole center. On top of this phase shift, we observed a shift in the vertical equilibrium position of the atoms in the TOP-trap. We achieved a high resolution of the equilibrium position by using very small condensate clouds and by exciting dipole oscillations of the cloud along the z -axis. Typical results of such measurements for the two senses of rotation of the bias field are shown in Fig. 3. Fitting a sinusoidal curve to the position data we determined the absolute centre of the oscillations to within $5 \mu\text{m}$ and the relative position of the centers to within $3 \mu\text{m}$. Identical conditions for both senses of rotation were ensured by powering the bias coils

from two phase-locked signal generators and shifting their relative phase by 180 degrees to reverse the sense of rotation whilst keeping all other parameters constant.

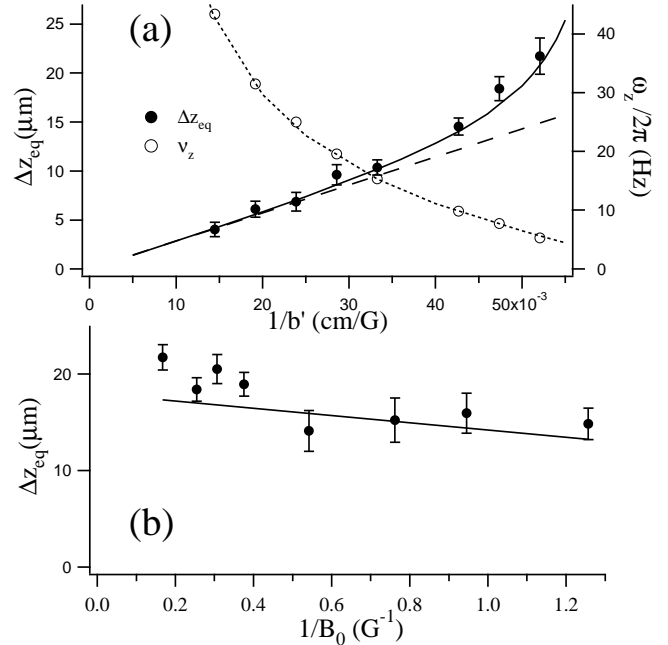


FIG. 4. (a) shows the dependence on the quadrupole gradient b' of the splitting Δz_{eq} of the equilibrium positions (filled symbols) for opposite senses of rotation of the bias field, and dependence of the oscillation frequencies (open symbols). The solid and dotted lines are the results of a numerical simulation *without* the adiabatic approximation. The dashed line is the prediction of Eq. 4; $B_0 = 4 \text{ G}$ for all points. In (b) we plot the dependence of the splitting (symbols: data, solid line: numerical simulation) on the inverse of the bias field strength for fixed gradient ($b' = 20 \text{ G cm}^{-1}$).

The measured dependence of the spatial separation Δz_{eq} of the two equilibrium positions on the inverse of the quadrupole gradient, $1/b'$, is shown in Fig. 4 (a). For large gradients, we find a linear dependence of Δz_{eq} on $1/b'$, whereas for the smallest gradients the splitting data deviate significantly from a straight line as b' approaches the minimum gradient, $b'_{\text{min}} = 15.3 \text{ G cm}^{-1}$, necessary to balance gravity. In Fig. 4 (b) the measured dependence of Δz_{eq} on the inverse of the bias-field B_0 is shown. Also plotted in Fig. 4 (a) is the dependence of ω_z on $1/b'$, allowing a calibration of b' with an accuracy of two percent over a very large range.

We have solved numerically the coupled differential equations of [10] for the center of mass motion and atomic spin within our TOP trap field. The numerical simulations provided an excellent fit for the results of Fig. 4 [14]. To find the equilibrium position, a transient damping was introduced in the numerical integration of the evolutions for the center-of-mass and/or the spin. We

have verified that damping rates corresponding to the trap lifetime do not modify the atomic micromotion and the non-adiabatic effects. However the role of additional damping mechanisms, for instance the viscous heating of [2], should be tested.

To interpret the dependence of the splitting Δz_{eq} on the field gradient, a transformation to a frame rotating synchronously with the bias field may be applied, as in [9,10]. For the special case of a cylindrical TOP trap this transformation completely removes the time dependence. The frame rotation acting on the spin variables introduces a fictitious (geometric) magnetic field $\mathbf{B}_g = -m_F \hbar \omega_0 \mathbf{k} / \mu$ along the rotation axis, with $m_F \hbar$ the atomic internal angular momentum. In a refined adiabatic approximation the spin is aligned with the effective field, i.e. the sum of the real and geometric magnetic fields. The occurrence of transverse components of the the spin with respect to the real magnetic field lies at the heart of the concept of geometric forces. The geometric field shifts vertically the plane of the quadrupole orbit. The difference Δz_{eq} in the equilibrium positions for cw and ccw rotations of the bias field is

$$\Delta z_{\text{eq}} = 2 \frac{m_F \hbar |\omega_0|}{\mu b'}. \quad (4)$$

Gravity shifts the equilibrium position z_{eq} downwards, but for a cylindrical trap the above result for Δz_{eq} is not modified. The expressions for the geometric force of [5] give rise to an equivalent result for the geometric field and the splitting Δz_{eq} . While for the cylindrical TOP trap the transformation to the rotating frame takes care completely of the spin dynamics, for the triaxial TOP trap the rotating frame transformation does not result in a time-independent problem. In fact, at low b' values, approaching b'_{min} , the splitting data of Fig. 4(a) deviate from the behavior described by Eq. (4). Higher order geometric terms derived in [5] lead to corrections several orders of magnitude too small to explain these deviations. Numerically we found that at zero gravity also for the triaxial TOP trap Δz_{eq} is well described by Eq. (4). This leads us to conjecture that gravity modifies the fast correlation between spin orientation and center-of-mass motion responsible for the geometric forces.

In summary, in a TOP trap the micromotion and the splitting of the equilibrium positions of the atoms for oppositely rotating bias fields are accounted for by a lifting of the time-average and adiabatic approximations. The dependence of the splitting on the magnetic field gradient arises from the nonadiabatic characteristics of the TOP trap. The micromotion in a TOP-trap is of relevance for experiments where an accurate control of the condensate residual motion on the recoil velocity scale (5 mm s^{-1}) is required, e.g. in atom lasers or condensate transfer. The observed dependence of the equilibrium position on the bias field rotation hopefully motivates theoretical efforts to calculate higher order corrections to

the adiabatic spin evolution in the TOP-trap configuration. Finally it should be tested, theoretically and experimentally, whether the condensate response to the parallel transport of the atomic spin in a TOP trap, which gives rise to the geometric forces, may influence also the internal dynamics of the condensate.

We thank G. Smirne for help in the data acquisition. O.M. gratefully acknowledges financial support from the European Union (TMR Contract-Nr. ERBFMRXCT960002). This work was supported by the INFM “Progetto di Ricerca Avanzata”, and by the CNR “Progetto Integrato”.

-
- [1] Recent reviews by W. Ketterle, *et al.*, and by E. Cornell, *et al.* in *Bose-Einstein condensation in atomic gases*, edited by M. Inguscio, S. Stringari and C. Wieman (IOS Press, Amsterdam) 1999.
 - [2] W. Petrich, *et al.*, Phys. Rev. Lett. **74**, 3353 (1995).
 - [3] E.W. Hagley, *et al.*, Science **283**, 1706 (1999).
 - [4] M.V. Berry, in *Geometric Phases in Physics*, edited by A. Shapere and F. Wilczek (World Scientific, Singapore, 1989) pp. 1-28.
 - [5] Y. Aharonov and A. Stern, Phys. Rev. Lett. **69**, 3593 (1992); R.G. Littlejohn and S. Weigert, Phys. Rev. A **48**, 924 (1993); M.V. Berry and J.M. Robbins, Proc. Roy. Soc. London Ser. A **442**, 641 (1993); M.V. Berry, *ibid.* **452**, 1207 (1996).
 - [6] V.I. Yukalov, Phys. Rev. A **56**, 5004 (1997); V.E. Shapiro, *ibid.* **60**, 719 (1999).
 - [7] A.B. Kuklov, *et al.*, Phys. Rev. A **55**, 488 (1997); V.G. Minogin, *et al.*, *ibid.* **58**, 3138 (1998).
 - [8] We used condensates mainly because their small size greatly facilitated precise position measurements. Experiments with evaporatively cooled thermal clouds yielded the same results within the experimental uncertainty.
 - [9] The rotation sensitive condensate position was discussed by D.S. Hall, *et al.*, Proc. SPIE **3270**, 98 (1998). It is also contained implicitly in the analytical model of [10].
 - [10] S. Gov and S. Shtrikman, J. Appl. Phys. **86**, 2250 (1999).
 - [11] TOP traps have been used for BEC in [2,3] and by D.J.Han, *et al.*, Phys. Rev. A **57** R4114 (1998); J.L. Martin, *et al.*, J. Phys. B: Atom. Mol. Opt. Phys. **32**, 3065 (1999); J. Arlt, *et al.*, *ibid.* **32** 5861 (1999).
 - [12] J.H. Müller, *et al.* J. Phys. B: Atom. Mol. Opt. Phys. in press and condmat/0005133.
 - [13] The switch-off time of the bias field, limited by the quality factor of tank circuits was around $150 \mu\text{s}$. However, fast switching of the bias field was not required as the atoms are no longer trapped once the quadrupole field is extinguished.
 - [14] We should mention that the agreement between simulations and experiments becomes less satisfactory for very elliptical bias field in the $x - y$ plane.